

Searches in CMS for new physics in final states with jets

Eirini Tziaferi on behalf of the CMS Collaboration

*National and Kapodistrian University of Athens,
157 72, Athens , Greece*

E-mail: e.tziaferi@cern.ch

Many new physics models, e.g., compositeness, extra dimensions, extended Higgs sectors, supersymmetric theories, and dark sector extensions, are expected to manifest themselves in final states with hadronic jets. This document presents searches for new phenomena in final states that include jets, focusing on the recent results obtained using the full Run-II data-set collected with the CMS experiment at the CERN LHC.

*41st International Conference on High Energy physics - ICHEP2022
6-13 July, 2022
Bologna, Italy*

1. Introduction

The motivation of the searches which will be discussed in this document is the potential for discovering physics beyond the standard model (SM). Many models of physics that extend the SM often require new particles that couple to quarks and/or gluons and decay to jets. The presented analyses use proton-proton collision data collected at $\sqrt{s} = 13$ TeV by the CMS experiment [1] at the CERN LHC Run-II period, corresponding to an integrated luminosity of 138 fb^{-1} .

2. Search for vector boson fusion production of same-sign muons through Majorana neutrinos or the Weinberg operator

This search considers models that generate neutrinos through two vector boson fusion (VBF) processes: the Majorana t-channel process which is mediated by a heavy (TeV-scale) neutrino (N) and the Weinberg operator t-channel process which is mediated by a lighter neutrino. The search for t-channel paves the way for discovering heavier neutrino masses since the cross-section of VBF t-channel process decreases more slowly with increasing mass compared with the usual neutrino hunting strategy searching for s-channel.

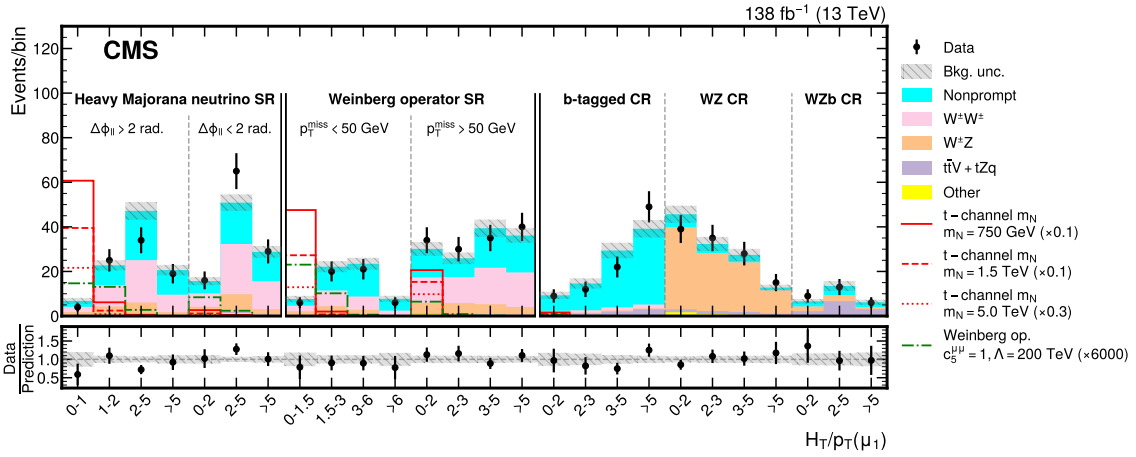


Figure 1: The $H_T/p_T(\mu_1)$ distribution in the SRs and CRs. The predicted yields of the backgrounds are shown with their best fit normalizations from the simultaneous fits for the background-only hypothesis. The lines indicate the scaled expected distributions of the heavy Majorana neutrino process for several N masses, and of the Weinberg operator process [2].

The experimental signature is two same-sign muons and two jets. Two signal regions (SRs) are defined for the two VBF processes in bins of $\Delta\phi_{11}$ and p_T^{miss} as shown in Fig. 1. The main background is WZ production and non-prompt leptons which are estimated through control regions (CRs). The main observable is the variable $H_T/p_T(\mu_1)$ since hadronic activity is typically suppressed in VBF production processes. Consequently, this variable has smaller values for signal events than for background events.

The maximum likelihood fit in $H_T/p_T(\mu_1)$ is performed simultaneously for both SRs and CRs

and upper limits on the N mixing element at the 95% CL as a function of the N mass are set as shown in Fig. 2. This is the first Majorana neutrino search reaching very high masses up to 23 TeV. For comparison, previous searches at s -channel (with dashed lines) are shown which reach up to 1 TeV. In addition, this analysis sets upper limit on effective $\mu\mu$ Majorana mass associated with the Weinberg operator exceeding the current best limit from Kaon experiments.

3. Search for high-mass resonances decaying to a jet and a Lorentz-boosted resonance

This analysis probes an unexplored, so far, LHC channel searching for high-mass hadronic resonances that decay to a parton (P3) and a Lorentz-boosted resonance (R2), which then decays into a pair of partons (P1,P2): $pp \rightarrow R1 \rightarrow R2 + P3 \rightarrow (P1 + P2) + P3$. The benchmark model which we consider is warped extra dimensions where R1 is a KK gluon (GKK) and R2 a radion (ϕ) ([3] and references therein).

The boosted resonance is reconstructed as a single wide cone jet R_{jet} with substructure consistent with a two-body decay, so the high-mass resonance is considered as a dijet system. The experimental signature is two wide cone resolved jets, one coming from R_{jet} and one coming from the third parton, P_{jet} . For maximum signal sensitivity the events are divided into several categories in a 2D plane as shown in Fig. 3 (left). The main background is multijet QCD production estimated with a data-driven method, using several parametric functional forms. The discrimination between signal and QCD background is achieved by exploiting jet substructure information (N-subjettiness ratio τ_{21}) and the kinematics of the decay. The former made possible the exploration of such a channel.

The maximum likelihood fit in the dijet masses is performed in all the categories simultaneously and upper limits on the product of cross-section and branching ratio (decay in to three gluons) are set in the 2D plane of Fig. 3 (right). The most significant excess in the data, when interpreted as a signal with $m(\text{GKK})=2.9$ TeV and $m(\phi)=0.4$ TeV, corresponds to a local significance of 3.2 standard deviations (σ). In this figure, results from the most recent CMS high-mass dijet search [4] are also shown (red lines) proving that the current search exploring a new experimental signature markedly extends the experimental exclusion of this new physics benchmark model.

4. Search for resonant and nonresonant production of pairs of dijet resonances

The paired dijet analysis searches for the pair-production of new particles decaying to two jets, resulting in a four-jet final state. The considered production modes are i) the resonant mode with the

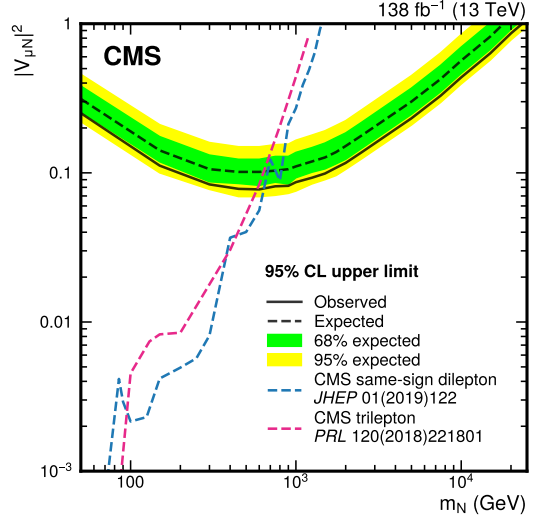


Figure 2: Upper limits on the heavy neutrino mixing element at the 95% CL as a function of the heavy neutrino mass m_N [2].

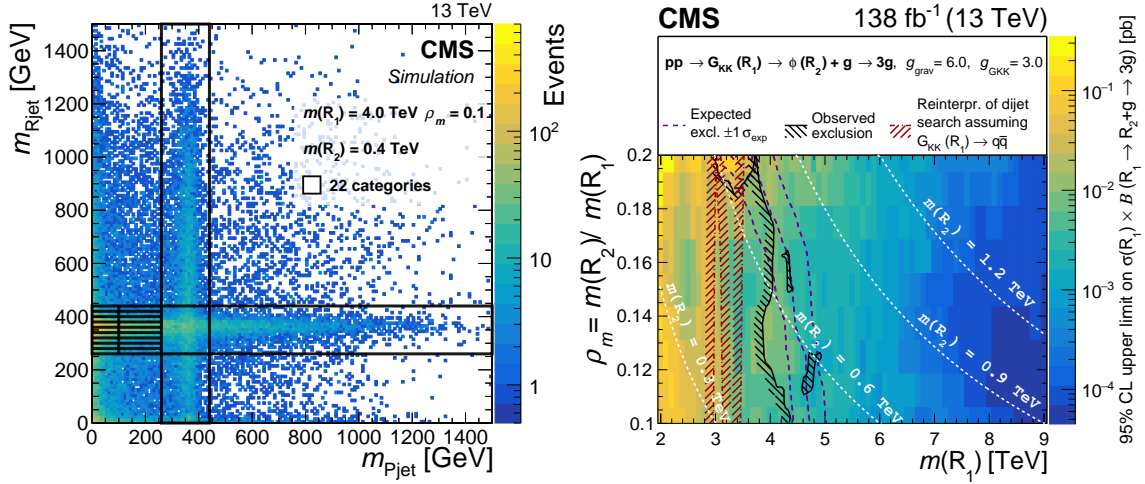


Figure 3: Left: The 2D plane of the reconstructed mass of the R2 jet candidate ($m_{R_{jet}}$) vs. mass of the P3 candidate ($m_{P_{jet}}$) for R_1 resonance events originating from a specific mass hypotheses. Right: Observed and expected upper limits on the product of signal cross-section and branching fraction, as a function of the ratio $\rho = m(R_2)/m(R_1)$ vs. $m(R_1)$, for a resonance model with three gluons in the final state [3].

benchmark model being a Diquark model ([5] and references therein) where a diquark S_{uu} decays in to vector-like quarks χ which then decay to a u quark and gluon and ii) the nonresonant mode with the benchmark model being an R-Parity Violating stop model ([5] and references therein) with stop pairs decaying to a d and s quark.

The resonant and nonresonant searches use two observables, the four-jet mass (m_{4j}) and the average dijet mass (\bar{m}_{jj}) respectively. We pair the leading four jets into two pairs exploring several pairing schemes in order to achieve the maximum expected signal significance. We define the variable $\alpha = \bar{m}_{jj}/m_{4j}$ which is a measure of the boost of the two dijet systems for both production modes. A localized excess is clearly visible in the 2D space of α vs. m_{4j} or \bar{m}_{jj} as shown in Fig. 4. The choice of this space was made in order to ensure that the fit distributions are not sculpted.

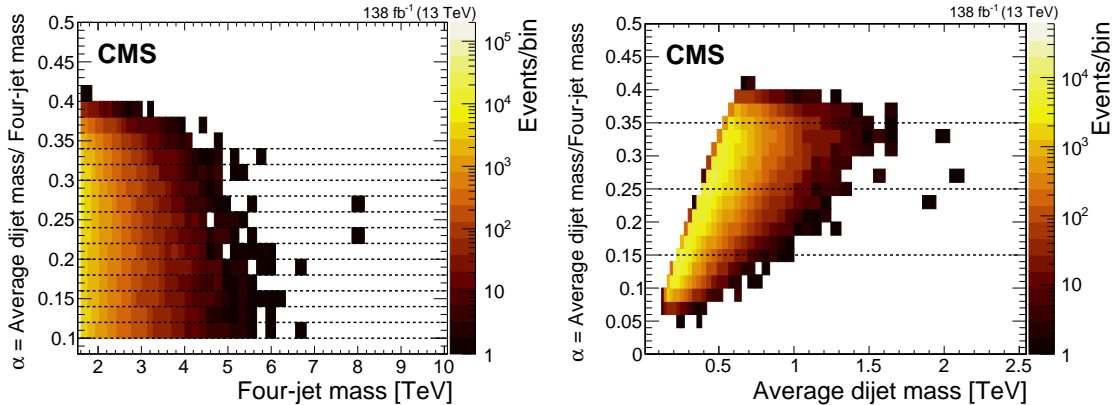


Figure 4: Left: Numbers of events observed within bins of the four-jet mass and the mass ratio α . Right: Numbers of events observed within bins of the average dijet mass and the mass ratio α .

Figure 5 depicts the event displays of the two highest four-jet mass events seen at the excess of Fig. 4. The main background of this analysis is the multijet QCD production estimated with a data-driven method using several functional forms.

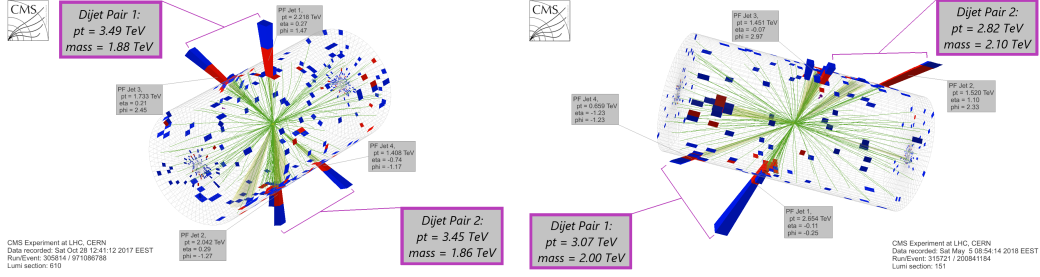


Figure 5: 3D displays of the events with the highest four-jet mass of 8.0 (left) and 7.9 (right) TeV.

The maximum likelihood fit in the four-jet mass and the average dijet mass is performed for the resonant and nonresonant search respectively. This is achieved with a set of 1D distributions that span the 2D space. Upper limits on the product of cross-section, branching ratio and acceptance are set. The local significance for resonant (nonresonant) production is 3.9 (3.6) σ . These are the first LHC limits on resonant pair production of dijet resonances via high mass intermediate states. In addition, the observed limits on nonresonant production significantly extend previous limits.

5. Search for leptoquarks decaying to a τ lepton and a b quark

This analysis searches for third-generation vector or scalar leptoquarks (LQs) coupling to a τ lepton and a b quark. It considers three production modes: single, pair production, and nonresonant production via t -channel LQ exchange. Pair production of LQs is independent of coupling strength λ , while single and nonresonant production are dependent and therefore we vary the coupling strength from 1 to 2.5. For high LQ masses the cross-section of the nonresonant production prevails over the other two production modes.

The experimental signature is two τ 's and one or two b jets. The fully hadronic, semi-leptonic channels, and the fully-leptonic channels are considered for estimating the main backgrounds which are $Z \rightarrow \tau\tau$, $t\bar{t}$, $j \rightarrow \tau_{fake}$. For the resonant production, the discriminating variable is S_T^{MET} which is the scalar sum of the p_T of the τ decay candidates, the leading jet p_T and p_T^{miss} . For the nonresonant production, the angular separation χ between the two τ leptons is used as discriminating variable. The choice of this variable is motivated by the fact that new physics processes with an isotropic distribution will appear as an excess at low values whereas the χ distribution in Rutherford scattering is flat.

A simultaneous maximum likelihood fit of LQ signals in χ and S_T^{MET} is performed. An excess in the χ distribution is seen and this is more visible in Fig. 6 (left) which shows a histogram with the number of events of χ and S_T^{MET} bins reordered and stacked by $\log_{10}[S/(S+B)]$, where S (B) is the total fitted signal (background) yield in a given bin. Upper limits are set on the third-generation LQ total (of all three modes) production cross-section for both vector and scalar LQs. Figure 6 (right) depicts the upper limits for a vector LQ assuming $\lambda = 2.5$. A 3σ excess can be seen, for masses greater than 1.8 TeV, which is mainly driven by the nonresonant mode.

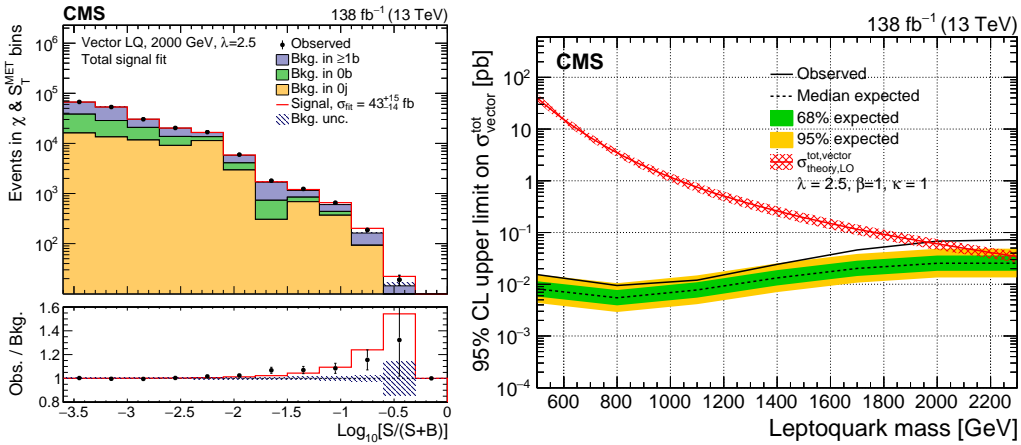


Figure 6: Left: Histogram of $\log_{10}[S/(S+B)]$ counting events in all bins, assuming a vector LQ with mass of 2000 GeV and $\lambda = 2.5$. Right: The observed and expected upper limit on the total cross-section of a vector LQ signal with $\lambda = 2.5$ at 95% CL [6].

6. Summary

The main analysis strategies and results of selected searches with jets in the final states using the full Run-II data-set collected with the CMS detector at the CERN LHC are discussed. Several intriguing excesses, with a local significance $> 3\sigma$, are observed on dijet, multijets and leptoquark searches with some channels and production modes explored for first time at LHC. With the increased center of mass energy and luminosity of Run III at LHC, along with improved analysis approaches, we should be able to fully exploit the discovery potential and either make a discovery or improve current limits.

References

- [1] CMS collaboration, *The CMS experiment at the CERN LHC*, *JINST* **3** (2008) S08004.
- [2] CMS collaboration, *Probing heavy Majorana neutrinos and the Weinberg operator through vector boson fusion processes in proton-proton collisions at $\sqrt{s} = 13$ TeV*, [2206.08956](#).
- [3] CMS collaboration, *Search for high-mass resonances decaying to a jet and a Lorentz-boosted resonance in proton-proton collisions at $\sqrt{s} = 13$ TeV*, *PLB* **1304** (2022) 137263.
- [4] CMS collaboration, *Search for high mass dijet resonances with a new background prediction method in proton-proton collisions at $\sqrt{s} = 13$ TeV*, *JHEP* **05** (2020) 033 [[1911.03947](#)].
- [5] CMS collaboration, *Search for resonant and nonresonant production of pairs of dijet resonances in proton-proton collisions at $\sqrt{s} = 13$ TeV*, *Submitted to JHEP* (2022) [[2206.09997](#)].
- [6] CMS collaboration, *The search for a third-generation leptoquark coupling to a τ lepton and a b quark through single, pair and nonresonant production at $\sqrt{s} = 13$ TeV*, *CMS-PAS-EXO-19-016* (2022) [<http://cds.cern.ch/record/2815309>].